

Initial-state energy loss in cold QCD matter and the Drell-Yan process

François Arleo^a, Charles-Joseph Naïm^{*a,b}, Stephane Platchkov^b

^a*Laboratoire Leprince-Ringuet, École polytechnique, CNRS/IN2P3, Université Paris-Saclay, 91128, Palaiseau, France*

^b*IRFU, CEA, Université Paris-Saclay, 91191 Gif-sur-Yvette, France*

E-mail: francois.arleo@cern.ch, charles-joseph.naim@cern.ch,
stephane.platchkov@cern.ch

ABSTRACT: The effects of parton energy loss in nuclear matter on the Drell-Yan process in pA and π A collisions at fixed-target energies are investigated. Calculations are based on the Baier-Dokshitzer-Mueller-Peigné-Schiff (BDMPS) framework embedded in a next-to-leading order calculation, using the transport coefficient extracted from J/ψ measurements. Model calculations prove in good agreement with preliminary measurements by the E906 experiment, despite a slightly different magnitude, supporting a consistent picture between Drell-Yan and J/ψ data. Predictions for the COMPASS future measurements in π A collisions at $\sqrt{s} = 18.9$ GeV are also performed. At higher collision energy ($\sqrt{s} = 38.7$ GeV), Drell-Yan measurements are only slightly affected by energy loss effects. On the contrary, the E906 results turn out in clear disagreement with nuclear PDF effects alone. The comparison of E772, E866, and E906 measurements indicates for the first time a clear violation of QCD factorization in Drell-Yan production in pA collisions.

KEYWORDS: cold QCD matter, parton energy loss

*corresponding author

Contents

1	Introduction	1
2	Drell-Yan production in hA collisions	4
2.1	NLO production cross section	4
2.2	Nuclear parton distribution functions	5
2.3	Initial-state energy loss	6
3	Phenomenology	7
3.1	E906 preliminary data	8
3.2	NA10 data	9
3.3	E866 data	10
3.4	Predictions for the COMPASS experiment	12
4	Violation of factorization in DY production in pA collisions	12
4.1	Factorization and x_2 scaling	12
4.2	x_2 scaling violation in the DY process	14
4.3	Comparing with J/ψ production	15
5	Summary	15

1 Introduction

The celebrated jet quenching phenomenon, observed in heavy ion collisions at RHIC and LHC, indicates that quarks and gluons experience radiative energy loss while propagating in a hot, deconfined QCD medium (see Refs. [1, 2, 3, 4] for recent reviews). The wealth of data collected so far has triggered detailed phenomenological studies serving a dual purpose, namely (i) to probe the radiative energy loss of partons (and multipartonic states) in a medium, and (ii) to extract the scattering properties of the expanding medium produced in these collisions, eventually leading to a better understanding of hot QCD matter.

Another way to study parton energy loss is to consider the production of hard QCD processes in hadron-nucleus (hA) collisions; see Ref. [5] for a recent discussion. In this case the medium, cold nuclear matter, is simpler: it is static with known size and nuclear density. It is not less interesting, though, as it reveals important features of medium-induced gluon radiation expected in QCD. More explicitly, hard processes

in hA collisions are sensitive to different timescales of gluon radiation: the Landau-Pomeranchuk-Migdal (LPM) regime, corresponding to gluon formation times of the order of the medium length ($t_f \lesssim L$), and the factorization regime (also known as *fully coherent*) for which $t_f \gg L$ [6].

The latter, fully coherent radiative energy loss, arises from the interference of gluon emission amplitudes off an ‘asymptotic’ incoming particle, produced long before entering the medium, and an asymptotic outgoing particle [7, 8, 9, 10, 11]. It thus differs from the initial-state (final-state) energy loss of a given incoming (outgoing) particle. In this regime, the average energy loss associated to the production of a massive particle (mass M) scales *linearly* with the particle energy E in the rest frame of the medium, [10]

$$\langle \epsilon \rangle_{\text{coh}} \propto (C_R + C_{R'} - C_t) \cdot \frac{\sqrt{\hat{q}L}}{M} \cdot E, \quad (1.1)$$

where C_R , $C_{R'}$ and C_t are respectively the color charge (Casimir) of the incoming, outgoing and exchanged¹ particle ($C_R = 4/3$ for a quark and $C_R = 3$ for a gluon), and \hat{q} is the transport coefficient of cold nuclear matter. The fully coherent energy loss could play a key role in the suppression of hard processes in hA collisions. It was shown in particular that this sole process is able to reproduce J/ψ suppression data in hA collisions [9, 12], from SPS to LHC energy and on a wide range in Feynman- x (x_F), in contradistinction to other effects such as nuclear modifications of parton distribution functions.

On the contrary, initial-state (or, final-state) energy loss is only sensitive to the LPM regime [10], for which the average energy loss is independent of the parton energy (up to a logarithmic dependence), [6]

$$\langle \epsilon \rangle_{\text{LPM}} \propto C_R \cdot \hat{q}L^2 \quad (1.2)$$

where now C_R is the Casimir of the propagating particle. The fact that the LPM fractional energy loss, $\langle \epsilon \rangle_{\text{LPM}}/E$, vanishes in the high energy limit has important consequences for the phenomenology. In particular, the effects of initial-state (or, final-state) energy loss in nuclear matter should be negligible in hA collisions at high energy, $\langle \epsilon \rangle_{\text{LPM}} \ll E$, as the particle energy *in the nucleus rest frame* gets large, $E \propto \sqrt{s}$.

Unless the particle energy becomes very small, $E \lesssim M\sqrt{\hat{q}L^3}$, the fully coherent energy loss exceeds that in the LPM regime, $\langle \epsilon \rangle_{\text{coh}} \gg \langle \epsilon \rangle_{\text{LPM}}$. However, not all processes are sensitive to fully coherent energy loss. One such case is particle production at large angle² (with respect to the beam axis) in the medium rest frame:

¹between the projectile hadron and the target nucleus

²At large angle, gluon emissions along the incoming parton and along the outgoing parton would not overlap, thus suppressing interferences.

this typically corresponds to the case of jet quenching in heavy ion collisions. Consequently, an energetic parton propagating in a hot medium is expected to experience final-state energy loss according to the LPM regime, Eq. (1.2). On the contrary, a particle produced in hA collisions is almost always produced with a large rapidity in the nucleus rest frame, thus at a ‘small’ angle, making it potentially sensitive to fully coherent energy loss [7]. Another process should be insensitive to fully coherent energy loss, namely the single inclusive production of Drell-Yan (DY) lepton pairs, since at leading order the final state is color neutral and therefore does not radiate gluons.³ Hence, the production of DY pairs in hA collisions appears as a promising candidate in order to probe LPM initial-state energy loss in cold nuclear matter.⁴ At next-to-leading order (NLO), the production of a virtual photon in association with a hard parton in the final state would make DY production potentially sensitive to fully coherent radiation; however, the dominant NLO subprocess at large x_F is Compton scattering, $qg \rightarrow q\gamma^*$, for which the fully coherent radiation is small ($\propto 1/N_c$) and negative.⁵ Final-state energy loss in nuclei could also be probed from the measurements of hadron production in semi-inclusive deep inelastic scattering (SIDIS) events [15, 16]. These processes are summarized in Table 1.

Energy loss	Process	Regime	$\langle\epsilon\rangle$
Initial-state	$hA \rightarrow \ell^+\ell^- + X$ (LO Drell-Yan)	$t_f \lesssim L$ (LPM)	$\propto \hat{q}L^2$
Final-state	$eA \rightarrow e + h + X$ (SIDIS)	$t_f \lesssim L$ (LPM)	$\propto \hat{q}L^2$
Fully coherent	$hA \rightarrow [Q\bar{Q}(g)]_8 + X$ (quarkonium)	$t_f \gg L$ (fact.)	$\propto \sqrt{\hat{q}L}/M \cdot E$

Table 1. Probing energy loss in cold nuclear matter in different processes.

Until now, the interpretation of DY data in hA collisions has been delicate and ambiguous. The E772 and later the E866 experiment at FNAL performed high-statistics measurements of DY pairs in pA collisions at $\sqrt{s} = 38.7$ GeV, on a wide range in x_F , $0.1 \lesssim x_F \lesssim 0.9$ [17, 18]. The depletion observed in heavier nuclei (Fe, W) at large x_F could either be attributed to nuclear parton distribution (nPDF) effects, namely sea quark shadowing at $x_2 \gtrsim 10^{-2}$ [19, 20, 21] or to strong energy loss effects in cold nuclear matter [22, 23, 24], therefore preventing a clear interpretation

³This can be seen from Eq. (1.1): in the DY case, $C_{R'} = 0$ and $C_R = C_t$, leading to a vanishing color prefactor.

⁴At high collision energy, e.g. at RHIC or LHC, LPM initial-state energy loss in nuclear matter is negligible, making DY production in pA collisions an ideal process to probe nuclear parton densities [13].

⁵In addition, these small effects could be balanced by the real NLO annihilation process, $q\bar{q} \rightarrow \gamma^*g$, significantly suppressed compared to Compton scattering [14] but more sensitive to fully coherent radiation ($\propto N_c$) and positive [10].

of these data. Older and less precise NA3 data in πA collisions at $\sqrt{s} = 16.8$ GeV [25] proved less sensitive to nPDF effects and allowed for setting upper limits on parton energy loss in nuclei; however these measurements were also compatible with vanishing parton energy loss [26]. Therefore, because of both the poorly known sea quark shadowing and the large experimental uncertainties in earlier data, no clear evidence for parton energy loss in the Drell-Yan process has yet been found. Two fixed-target experiments now make it possible to better understand the origin of the DY nuclear dependence. The E906 experiment [27] recently performed preliminary measurements of DY production in pA collisions at $\sqrt{s} = 15$ GeV on a wide range of x_F [28]. In addition, the COMPASS experiment at the SPS collected data in πA collisions at $\sqrt{s} = 18.9$ GeV that could be used to determine DY nuclear production ratios also on a large x_F interval [29].

The goal of this article is to revisit the effects of LPM initial-state energy loss in the BDMPS formalism on DY production in hA collisions at fixed target energies ($\sqrt{s} < 40$ GeV), with a systematic comparison between model calculations and experimental results. The theoretical framework is presented in Section 2 and results are shown in Section 3. The violation of QCD factorization in Drell-Yan production in pA collisions is discussed in Section 4. Conclusions are drawn in Section 5.

2 Drell-Yan production in hA collisions

2.1 NLO production cross section

We consider the inclusive production of Drell-Yan lepton pairs of large invariant mass, $M \gg \Lambda_{\text{QCD}}$, in hadronic collisions. The analysis is carried out at next-to-leading order accuracy in the strong coupling constant, i.e. at order $\mathcal{O}(\alpha^2 \alpha_s)$, using the DYNNLO Monte Carlo program [30, 31]. The x_F -differential production cross section in a generic $h_1 h_2$ collision reads

$$\frac{d\sigma(h_1 h_2)}{dx_F dM} = \sum_{i,j=q,\bar{q},g} \int_0^1 dx_1 \int_0^1 dx_2 f_i^{h_1}(x_1, \mu_R^2) f_j^{h_2}(x_2, \mu_R^2) \frac{d\hat{\sigma}_{ij}}{dx_F dM}(x_1 x_2 s, \mu^2, \mu_R^2). \quad (2.1)$$

At NLO, the partonic cross section $\hat{\sigma}_{ij}$ includes Compton scattering and annihilation processes, $qg \rightarrow q\gamma^*$ and $q\bar{q} \rightarrow g\gamma^*$, in addition to virtual corrections to the Born diagram, $q\bar{q} \rightarrow \gamma^*$. In Eq. (2.1), both the renormalization and factorization scales are set equal to the DY invariant mass,⁶ $\mu_R^2 = \mu^2 = M^2$. The single differential cross section $d\sigma/dx_F$ is obtained by integrating (2.1) over the dilepton mass range, here between the charmonium and bottomonium resonances.

In this analysis we are interested in the production of Drell-Yan pairs using either a proton or a pion beam on nuclear targets, pA and πA collisions. In the absence

⁶In the following, the explicit scale dependence is omitted for clarity.

of genuine nuclear effects, $f_j^{\text{h}2}$ appearing in Eq. (2.1) should thus be replaced by the corresponding average over proton and neutron partonic densities,

$$f_j^A(x_2) = Z f_j^p(x_2) + (A - Z) f_j^n(x_2) \quad (2.2)$$

where Z and A are respectively the atomic and the mass number of the nucleus A . Several proton NLO PDF sets have been used in this analysis (MMHT2014 [32], nCTEQ [20], and CT14 [33]) in order to evaluate part of systematic uncertainties of our calculations. The GRV NLO set [34] has been used for the PDF in a pion (we checked that the SMRS [35] and BSMJ [36] sets give almost identical results). The neutron parton distributions are deduced from those in a proton using isospin symmetry, $f_d^n = f_u^p$, $f_u^n = f_d^p$, $f_d^n = f_u^p$, $f_u^n = f_d^p$, and $f_i^n = f_i^p$ otherwise.

We are interested here in the nuclear dependence of the Drell-Yan process, via the production ratio,

$$R_h^{\text{DY}}(A/B, x_F) = \frac{B}{A} \left(\frac{d\sigma(\text{hA})}{dx_F} \right) \times \left(\frac{d\sigma(\text{hB})}{dx_F} \right)^{-1}, \quad (2.3)$$

in a heavy nucleus (A) over a light nucleus (B). In the absence of nuclear effects, Eq. (2.3) may differ from unity because of the differences between proton and neutron parton densities. In practice, proton-induced Drell-Yan collisions probe the target *antiquarks* for which $f_q^n \simeq f_q^p$, resulting in rather small isospin effects.⁷ Isospin effects are more important in low energy πA collisions, mostly sensitive to the valence up and down quark distribution in the nucleus.

2.2 Nuclear parton distribution functions

Parton distribution functions in a nucleus differ from those in a free proton over the whole Bjorken- x range, $f_i^{p/A}(x) \neq f_i^p(x)$, where $f_i^{p/A}$ is defined as the PDF of the parton of flavor i inside a proton bound in a nucleus. The latest global fit extractions of nPDF at NLO have been done by DSSZ [19], nCTEQ15 [20], and EPPS16 [21] which included for the first time data from the LHC.

In order to take into account nPDF effects on DY production, f_j^p (f_j^n) needs to be replaced by $f_j^{p/A}$ ($f_j^{n/A}$) in Eq. (2.2),

$$f_j^A(x_2) = Z f_j^{p/A}(x_2) + (A - Z) f_j^{n/A}(x_2). \quad (2.4)$$

Depending on the parametrizations, either the absolute PDF $f_j^{p/A}$ or the nPDF ratios, $R_j^A \equiv f_j^{p/A}/f_j^p$, are provided.

⁷The slight sea quark asymmetry is actually probed from the comparison of DY production in pp and pD collisions. Here, we shall always compare DY yields on nuclei with similar Z/A ratios, making this effect small (see Section 3.1).

In this article, DY production in pA and π A collisions is computed using the nPDF ratios provided by the latest nPDF set, EPPS16 [21]. This set actually includes DY data in both pA and π A collisions, in addition to other measurements. The implicit assumption is that no other physical effect than a universal leading-twist nuclear PDF would play a role in the production of DY pairs in hadron-nucleus collisions. However, the radiative energy loss of partons may affect the nuclear dependence of DY production, thus spoiling a clean extraction of nPDFs from these data.

2.3 Initial-state energy loss

The high-energy partons from the hadron projectile experience multiple scattering while propagating through nuclear matter. This rescattering process induces soft gluon emission, carrying away some of the parton energy available for the hard QCD process, here the Drell-Yan mechanism. The effects of initial-state energy loss on DY can be modelled as [26]

$$\begin{aligned} \frac{d\sigma(hA)}{dx_F dM} = & \sum_{i,j=q,\bar{q},g} \int_0^1 dx_1 \int_0^1 dx_2 \int_0^{(1-x_1)E_b} d\epsilon \mathcal{P}_i(\epsilon) f_i^h \left(x_1 + \frac{\epsilon}{E_b} \right) f_j^A(x_2) \\ & \times \frac{d\hat{\sigma}_{ij}}{dx_F dM}(x_1 x_2 s), \end{aligned} \quad (2.5)$$

where E_b is the hadron beam energy in the rest frame of the nucleus, and \mathcal{P}_i is the probability distribution in the energy loss of the parton i [37]. The latter has been determined numerically from a Poisson approximation [38, 39], using the LPM medium-induced gluon spectrum derived by Baier-Dokshitzer-Mueller-Peigné-Schiff (BDMPS) [40]. The first moment of this distribution is given by

$$\langle \epsilon_i \rangle \equiv \int d\epsilon \epsilon \mathcal{P}_i(\epsilon) = \frac{1}{4} \alpha_s C_R \hat{q} L^2 \quad (2.6)$$

where $\alpha_s = 1/2$ is frozen at low scales, $\hat{q}L \lesssim 1$ GeV². The medium length L is given by $L = 3/4R$ with $R = r_0 A^{1/3}$ is the nuclear radius, assuming a hard sphere nuclear density profile ($r_0 = (4\pi\rho/3)^{-1/3} = 1.12$ fm and ρ is the nuclear matter density).

The transport coefficient has been parametrized as (see appendix of Ref. [9])

$$\hat{q}(x) \equiv \hat{q}_0 \left(\frac{10^{-2}}{x} \right)^{0.3} ; \quad x = \min(x_0, x_2) ; \quad x_0 \equiv \frac{1}{2m_p L}, \quad (2.7)$$

where the power law behavior reflects the x -dependence of the gluon distribution in the nucleus at small values of x . In this article we shall consider DY production in low energy hA collisions, probing large values of x_2 , typically $x_2 > x_0$. Therefore, the transport coefficient used in (2.6) is essentially frozen at x_0 , $\hat{q}(x_0) = (0.02 m_p L)^{0.3} \hat{q}_0 \simeq 0.8 \hat{q}_0$ in a large nucleus ($L = 5$ fm). The coefficient \hat{q}_0 is the only

parameter of the model. It has been determined from J/ψ data using the energy loss in the fully coherent regime, $\hat{q}_0 = 0.07\text{--}0.09 \text{ GeV}^2/\text{fm}$ [9]. No attempt has been made here to extract an independent estimate of \hat{q} from low energy DY data, as the measurements from the E906 experiment are still preliminary. Eventually, this would allow one to check the universality of this parameter, for different processes and in different energy loss regimes (LPM for DY, fully coherent for J/ψ ; see Introduction).

The BDMPS formalism is particularly suited to describe gluon radiation induced by multiple soft scattering, thus appropriate for thick media for which the typical number of scatterings, $n = L/\lambda$, is large (λ is the parton mean free path). This is at variance with the GLV [41] and higher-twist approach [42], which instead consider a single hard scattering in a medium. Using $\hat{q} = \mu^2/\lambda$, where $\mu \simeq 200 \text{ MeV}$ is the typical momentum transfer in single soft scattering, the number of scatterings in a big nucleus (taking $L = 5 \text{ fm}$) is $n = \hat{q}L/\mu^2 = 7\text{--}9$, which is consistent with the initial assumption of BDMPS.⁸

As can be seen from Eq. (2.5), the nuclear dependence of DY production depends on the shape of the hadron beam PDF: the steeper the x -dependence of f_i^h , the stronger the DY suppression. Since at large x one expects $f_q^p(x) \sim (1-x)^3$ and $f_q^\pi(x) \sim (1-x)^2$ from quark counting rules [43], a stronger DY suppression can be expected in pA collisions with respect to that in π A collisions [26]. Another consequence follows from Eq. (2.5). At large x_F , the maximal amount of parton energy loss is restricted to be $\epsilon < (1-x_1) E_b \simeq (1-x_F) E_b$, making DY production dramatically suppressed at the edge of phase-space, $x_F \lesssim 1$.

3 Phenomenology

On top of isospin effects (labelled CT14 in the figures), the DY nuclear production ratio (2.3) is computed assuming either nPDF effects, as estimated using the EPPS16 parton densities in Eq. (2.2) and their associated error sets, or initial-state energy loss effects, Eq. (2.5). Although each effect is here studied separately, both could in principle be taken into account in order to achieve a complete description of the Drell-Yan process in hA collisions.

The calculations are compared to the preliminary results from E906⁹ at $E_p = 120 \text{ GeV}$ [28], NA10 data at $E_{\pi^-} = 140 \text{ GeV}$ [44] and E866 at $E_p = 800 \text{ GeV}$ [18]. Predictions for the COMPASS experiment, which are being collected Drell-Yan data in π A collisions at $E_{\pi^-}=190 \text{ GeV}$ [29], are also presented.

⁸Note that in a single hard picture, the momentum transfer needs to be large enough in order to induce gluon emission. Taking $\mu_{\text{semi-hard}} \simeq 500 \text{ MeV}$ leads to $n \simeq 1$, also consistent with the assumption of a small number of (semi-hard) scattering.

⁹These are not included in the global fit of EPPS16.

3.1 E906 preliminary data

The preliminary results from the E906 experiment [27, 28] on the ratios $R_{\text{pA}}(\text{Fe/C})$ and $R_{\text{pA}}(\text{W/C})$ are shown as a function of x_{F} in Fig. 1. The mass range is $4.5 < M < 5.5$ GeV at $\sqrt{s} = 15$ GeV with an additional kinematical cut, $0.1 < x_2 < 0.3$.

The data indicate a clear DY suppression in both Fe and W nuclear targets, increasingly pronounced at large x_{F} , in clear contrast with the nPDF calculations shown as a blue band. In particular, nPDF effects make R_{pA} consistent with the CT14 predictions assuming no nuclear modification of parton densities, see (2.1), shown as a dashed line in Fig. 1. This x_{F} range indeed corresponds to typical values of $x_2 \simeq 0.1\text{--}0.3$, at the boundary between the EMC effect and the antishadowing region, hence for which $f_i^{p/A} \simeq f_i^p$. The slight rise of R_{pA} with increasing x_{F} , seen for both CT14 and EPPS16, originates from the asymmetry in the nucleon sea, $f_d^p > f_u^p$.¹⁰ To our knowledge, this is the first time that DY measurements in hA collisions exhibit such a clear disagreement with the nPDF expectations.

The initial-state energy loss effects, assuming the default choice of $\hat{q}_0 = 0.07\text{--}0.09$ GeV²/fm, are shown as a red band. The model uncertainty includes the choice of different proton PDF sets, on top of the variation of \hat{q}_0 . The calculations predict a significant DY suppression which becomes more pronounced as x_{F} gets larger, in qualitative agreement with the E906 results. While the magnitude of R_{pA} is smaller in the measurements than in the model, by roughly 5% and 10% in W and Fe targets respectively, we find it nevertheless remarkable that the *shapes* of R_{pA} predicted by the energy loss model and the E906 results prove similar.¹¹ In our opinion, these preliminary data strongly hint at the existence of (LPM) initial-state quark energy loss in the DY process. The origin of the different magnitude in the data and in the model is not clear. We checked that a larger transport coefficient would reproduce perfectly the W/C ratio, however at the expense of a non-universal coefficient in the LPM and fully coherent energy loss regimes. Also, note that the present discrepancy is of the same order as the nPDF uncertainty; adding initial-state energy loss together with nPDF effects would thus come in good agreement with the data. Finally, it cannot be excluded that fully coherent energy loss, expected at NLO in the $q\bar{q} \rightarrow \gamma^* g$, could lead to an extra suppression at large x_{F} . Any conclusion nonetheless awaits for the E906 measurements to become final.

Earlier calculations have been performed in a different theoretical set-up, the higher twist (HT) formalism, which allows for computing within the same framework the DY production process and the energy loss effects, assuming one additional hard scattering in the target nucleus [45]. These calculations should match at leading twist (assuming no additional scattering) the leading order DY production cross sec-

¹⁰Thus in a W target, for which neutrons are more abundant than protons, one expects $f_u^{\text{W}} > A_{\text{W}} f_u^p$, leading to R_{pA} slightly above unity.

¹¹In particular, the calculation of R_{pA} does not depend on any free parameter.

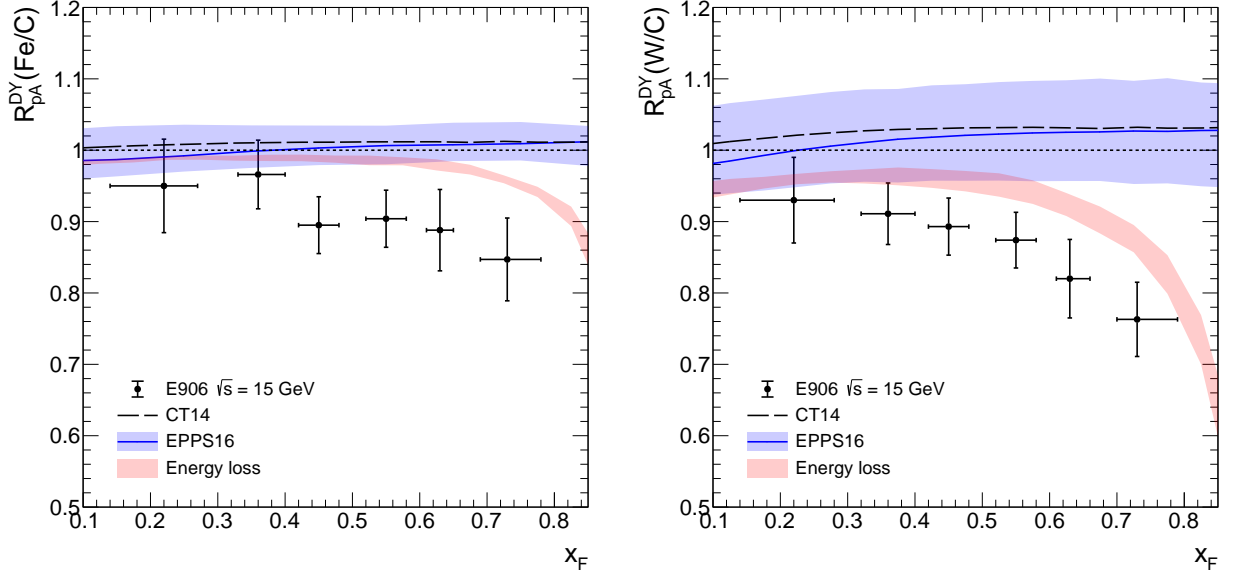


Figure 1. E906 nuclear production ratio measured in pFe (left) and pW (right), normalized to pC, collisions at $\sqrt{s} = 15$ GeV compared to EPPS16 nPDF calculation (blue band), isospin effect (dotted line) and energy loss effects (red band).

tion. On the contrary, the DY process is here computed at NLO accuracy to which a rescaling of the projectile PDF is assumed, in order to model energy loss effects arising from multiple soft scattering in the medium, see Eq. (2.5). Despite these important differences, both calculations of the DY nuclear production ratio prove remarkably similar (and the HT calculation of Ref. [45] in agreement with E906 preliminary data). It should also be mentioned that the transport coefficient used in both approaches coincide, as the *gluon* transport coefficient used here would correspond to a *quark* transport coefficient given by $\hat{q}_{\text{quark}} = 4/9 \hat{q} \simeq 0.025\text{--}0.032$ GeV²/fm (in a W nucleus) perfectly matches the value $\hat{q}_{\text{quark}} = 0.024 \pm 0.008$ GeV²/fm used in Ref. [45] and extracted from semi-inclusive DIS measurements [46].

3.2 NA10 data

The NA10 collaboration collected Drell-Yan data on two nuclear targets (W, D) and in the mass range is $4.35 < M < 15$ GeV at $\sqrt{s} = 16.2$ GeV, excluding the Υ peak region $8.5 < M < 11$ GeV.

The original measurements were corrected for isospin effects in the W target [44]. Similarly, an isospin correction [47] is applied to the present calculation, defined as

$$R_{\pi^-}^{\text{NLO-isospin corrected}}(\text{W/D}) = R_{\pi^-}^{\text{LO}}(\text{W}^{\text{isocalar}}/\text{W})_{\text{no nPDF}} \times R_{\pi^-}^{\text{NLO}}(\text{W/D}), \quad (3.1)$$

where $R_{\pi^-}^{\text{LO}}(\text{W}^{\text{isocalar}}/\text{W})_{\text{no nPDF}}$ is calculated at leading order in an ‘isospin-symmetrized’ W nucleus ($Z = A/2$) over that in a W nucleus. The isospin corrected nPDF calculation overestimates the data, as illustrated in Fig. 2. This disagreement has also been

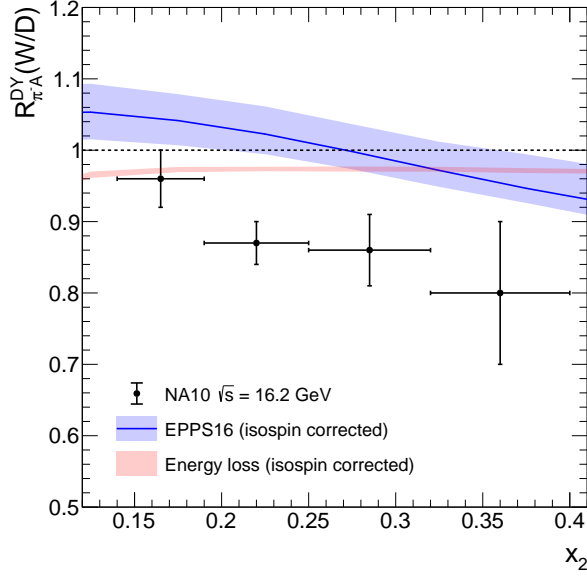


Figure 2. NA10 nuclear production ratio, corrected for isospin effects, measured in πW , normalized to πD , collisions at $\sqrt{s} = 16.2$ GeV compared to EPPS16 nPDF calculation (blue band) and energy loss effects (red band).

reported by Paakkinen et al. [47] who apply a rescaling factor of 12.5% ($r = 1.125$) in their calculations to make data and nPDF corrections come in agreement. This rescaling is however twice larger than the systematic uncertainties of 6% reported in the experiment [44].

The energy loss calculation shown in Fig. 2 leads to a suppression of approximately 3% ($R_{pA} \simeq 0.97$), independent of x_2 . As expected, energy loss effects in πA collisions turn out to be significantly smaller than in pA collisions due to the harder quark distribution in a pion with respect to that in a proton (see Section 2.3). Taking into account energy loss in addition to nPDF effects would thus require a rescaling factor of approximately $1.125 \times 0.97 = 9\%$, instead of 12.5% previously, hence closer to the reported experimental systematic uncertainty.

Perhaps more importantly, the present calculation shows that initial-state energy loss gives an effect on $R_{\pi A}$ of the same magnitude as that of nPDF corrections. This may thus question a reliable extraction of nuclear parton distributions from DY data in πA collisions without taking energy loss effects into account. Moreover, although $R_{\pi A}$ proved to be constant (but still different from unity) in this x_2 range, we shall see in Section 3.4 that it is not necessarily always the case.

3.3 E866 data

The E866 collaboration measured the Fe/Be and W/Be nuclear production ratios in pA collisions at $\sqrt{s} = 38.7$ GeV. The integrated mass range is $4 < M < 8$ GeV, with

an additional kinematical cut $0.02 \lesssim x_2 \lesssim 0.10$.

The nuclear depletion of DY production in E772 and E866 data has long been delicate to interpret as it is virtually impossible to disentangle both nPDF and energy loss processes from these sole measurements [26]. Several groups attribute the measurements as coming mostly from large energy loss effects [22, 23, 24], while the nPDF analyses instead assume energy loss effects to be negligible and hence do incorporate these experimental data in the global fits [19, 20, 21]. The comparison

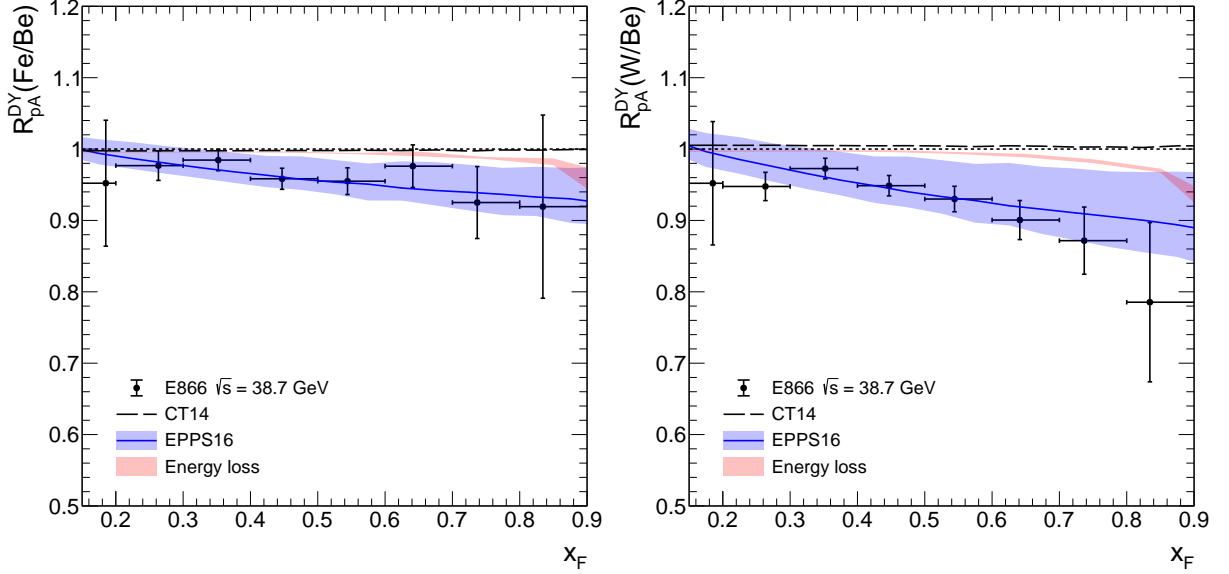


Figure 3. E866 nuclear production ratio measured in pFe (left) and pW (right), normalized to pBe, collisions at $\sqrt{s} = 38.7$ GeV compared to EPPS16 nPDF calculation (blue band), isospin effect (dotted line) and energy loss effects (red band).

between our results and the data is shown in Fig. 3. The agreement between nPDF calculation and the data is satisfactory for both nuclear ratios. However, this should not come as a surprise since these data have been used in the global fit of EPPS16. In Ref. [26], NA3 DY data in πA collisions were used at lower energy to extract an upper limit on the amount of quark energy loss in nuclear matter, and hence helped to lift this ‘degeneracy’ at E866 energy. That study led to the conclusion that energy loss effects on the E866 DY measurements were presumably small. Here, the independent estimate of \hat{q} from J/ψ suppression data – which are not included in nPDF analyses – corroborates this statement as parton energy loss shows a negligible effect, except at very large $x_F \gtrsim 0.8$ (see Fig. 3). At E866 energy and above, the forward DY measurements in pA collisions are therefore most likely due to nPDF effects and hence could be included in the global fit analyses.¹² At LHC, the coming DY mea-

¹²The extraction of sea quark nPDF at small $x_2 \sim 10^{-2}$ (corresponding the largest x_F bin in the experiment) is probably affected by a few percent.

measurements in pPb collisions at the LHC should thus allow for a clean extraction of nPDF at small x [13].

3.4 Predictions for the COMPASS experiment

Drell-Yan data are also being collected by the COMPASS collaboration at the CERN SPS, using a pion beam on two nuclear targets (NH_3 , W) at a collision energy $\sqrt{s} = 18.9$ GeV [29]. The expected mass range is $4.3 < M < 8.5$ GeV. With such a mass range, the COMPASS measurements would explore a typical range in $0.1 \lesssim x_2 \lesssim 0.5$, embracing both the antishadowing and EMC regions.

The predictions for the ratio $R_{\pi\text{A}}^{\text{DY}}(\text{W}/\text{NH}_3)$ are shown in Fig. 4. A significant suppression from isospin effects (dashed curve) are expected because of the lesser up quark density in W than in NH_3 nuclear target.¹³ Because of the valence quark antishadowing in the EPPS16 set, the inclusion of nPDF corrections increases $R_{\pi\text{A}}$ by up to 5% with respect to the calculation assuming no nuclear effect.¹⁴

On the contrary, energy loss effects would lead to a suppression of the DY yield, increasingly pronounced at larger x_F as the phase space available for gluon radiation shrinks. At $x_F = 0.9$, the model predicts a suppression of $R_{\pi\text{A}} \simeq 0.8$ while isospin effects only would lead to $R_{\pi\text{A}} \simeq 0.94$. Despite the smaller energy loss effects in πA collisions, the future DY measurements by the COMPASS experiment will provide additional constraints for the extraction of the transport coefficient, thanks to the large x_F acceptance and the expected statistics.

Before closing this section, let us mention that the pion PDF are extracted from DY production measured in pion-induced collisions on *nuclear* targets, assuming no nuclear effect beyond isospin corrections. However, energy loss effects may affect the reliable extraction of the pion PDF at large x , $f_u^\pi(x) \sim (1-x)^n$, and make n possibly overestimated in the PDF global fits. In order to estimate the error associated to the use of nuclear targets, the DY nuclear production ratio has been fitted as $R_{\pi\text{A}}(x_1) = (1-x_1)^{\delta n}$, where $\delta n \simeq 0.06$ is a typical correction to the slope of the pion PDF.

4 Violation of factorization in DY production in pA collisions

4.1 Factorization and x_2 scaling

It has been shown in the previous section that calculations using EPPS16 nPDF sets fail to describe the preliminary results by the E906 experiment (Fig. 1), while exhibiting a good agreement with E866 measurements (Fig. 3). It could be argued

¹³Using $Z_W/A_W \approx 2/5 \simeq 1 - Z_{\text{NH}_3}/A_{\text{NH}_3}$ leads to an expected suppression $R_{\pi\text{A}} \simeq (1 + 3/2r)/(3/2 + r) \approx 7/8$ assuming $r \equiv d/u \approx 1/2$ at large x_2 . At smaller x_2 , hence at larger x_F , r is getting larger and so does $R_{\pi\text{A}}$.

¹⁴The EMC region is probed at smaller values of x_F , not shown in Fig. 4.

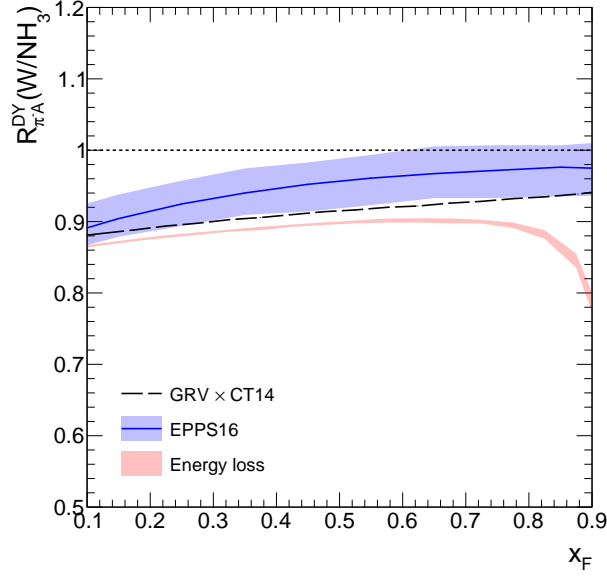


Figure 4. Nuclear production ratio measured in πW , normalized to πNH_3 , collisions at $\sqrt{s} = 18.9$ GeV compared to EPPS16 nPDF calculation (blue band), isospin effect (dotted line) and energy loss effects (red band)

that *this* specific nPDF set is unable to account for both data sets. On the contrary, we demonstrate here that the failure to describe both data sets should be generic to all calculations based on nPDF effects only, following the reasoning of Ref. [48].

Let us consider the factorized expression for the DY production cross section in pA collisions, Eq. (2.1), assuming possible nPDF corrections, Eq. (2.4). In the forward region, $x_F = x_1 - x_2 > 0$, and at large collision energy ($\hat{s}/s \simeq M^2/s \ll 1$), the momentum fractions carried by the incoming partons can be approximated as $x_1 \simeq x_F$ and $x_2 = \hat{s}/(x_F s)$. Since forward DY production is dominated by the scattering of a quark in the incoming proton, the pA differential cross section (2.1) can thus be approximated as [48]

$$\begin{aligned} \frac{d\sigma(\text{pA})}{dx_F dM} &\simeq f_q^p(x_F) \times \left(\sum_{j=q,\bar{q},g} \int dx_2 f_j^A(x_2) \frac{d\hat{\sigma}_{qj}}{dx_F dM}(x_F x_2 s) \right) \\ &\simeq f_q^p(x_F) \times \left(\sum_{j=q,\bar{q},g} f_j^A(x_2) \frac{d\hat{\sigma}_{qj}}{dx_F dM}(M^2) \right) \end{aligned} \quad (4.1)$$

where the second line is obtained assuming that the partonic cross section peaks close to the threshold, $\hat{s} \gtrsim M^2$.

Using Eq. (4.1), the nuclear production ratio (2.3) thus becomes a scaling function of the x_2 momentum fraction only – independent of the center-of-mass energy of the collision – should the factorization hold in DY forward production in pA collisions. Conversely, a lack of x_2 scaling in data would signal the breakdown of QCD

factorization and would indicate that nPDF corrections alone cannot account for the nuclear dependence of DY production.

4.2 x_2 scaling violation in the DY process

In order to check whether the DY nuclear production ratio indeed scales like x_2 , the pA data from E772 (on W/D targets), E866 (both taken at $\sqrt{s} = 38.7$ GeV) and E906 ($\sqrt{s} = 15$ GeV) are plotted as a function of x_2 in Fig. 5 (left). The comparison between E772 and E906 results clearly show a violation of x_2 scaling at large $x_2 \sim 10^{-1}$.¹⁵ On the contrary, it has been checked that the NLO calculations (using EPPS16 nPDF sets) at both energies follow, as expected, x_2 scaling to a very good accuracy.

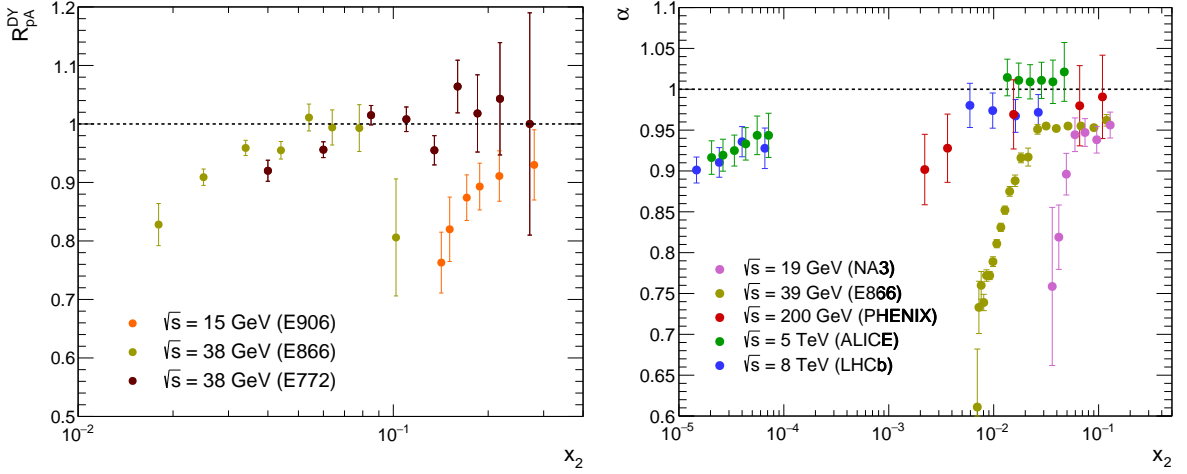


Figure 5. Left: DY nuclear production ratio measured by E772 [17], E866 [18], E906 [28], plotted as a function of x_2 . Right: Nuclear dependence of J/ψ production measured by NA3 [51], E866 [52], PHENIX [53], ALICE [54] and LHCb [55], plotted as a function of x_2 .

This comparison thus provides for the first time a clear evidence of the violation of QCD factorization in the Drell-Yan process in pA collisions, implying the presence of higher-twist processes. A natural candidate responsible for the reported violation of x_2 scaling is LPM initial-state energy loss, as the comparison between the model calculation and E906 results suggests. As mentioned in the Introduction, initial-state energy loss should have a weak impact at high incoming parton energy, $E = x_1 E_b = M^2/(x_2 s)$. Therefore, no violation of x_2 scaling in DY production is expected at small values of x_2 , as $\langle \epsilon \rangle_{\text{LPM}}/E \propto x_2$.

¹⁵In principle the backward ($-2.2 < y < -1.2$) DY data by PHENIX in pAu collisions at $\sqrt{s} = 200$ GeV could probe similar values of x_2 , yet the present uncertainties prevent any quantitative conclusions yet [49]. Similarly, future measurements by the LHCb experiment in pPb collisions at $\sqrt{s} = 8.16$ TeV [50] may also access the large x_2 domain.

4.3 Comparing with J/ψ production

Such x_2 scaling breakdown has long been reported in J/ψ production [48], later confirmed by measurements at higher collision energy [56]. Fig. 5 (right) shows the nuclear dependence of J/ψ production in pA collisions¹⁶ measured by NA3 [51], E866 [52], PHENIX [53], ALICE [54] and LHCb [55], from $\sqrt{s} \simeq 20$ GeV to $\sqrt{s} \simeq 8$ TeV. As can be seen, the J/ψ suppression data clearly rule out the x_2 scaling predicted by QCD factorization. This prevents the use of J/ψ measurements in pA collisions in order to extract nuclear parton densities.

The x_2 dependence of DY and J/ψ suppression at different collision energies show similar patterns, despite a clear difference in the magnitude of the suppression.¹⁷ In the case of J/ψ production, the good agreement between data and the model based on fully coherent energy loss [8, 9] makes the latter a natural process responsible for the breakdown of x_2 scaling. Unlike initial-state energy loss, fully coherent energy loss is proportional the parton energy, Eq. (1.1), making $\langle\epsilon\rangle_{\text{coh}}/E$ independent of x_2 . As a consequence, quarkonium suppression should not follow x_2 scaling even at small values of x_2 .

5 Summary

The effects of parton energy loss on Drell-Yan production in pA and π A collisions at fixed-target energies has been investigated, based on a BDMPS energy loss framework embedded in a NLO calculation. Nuclear production ratios were compared to calculations assuming nPDF effects as well as to experimental results. Let us summarize the main conclusions of this study:

- Preliminary results by the E906 experiment in pA collisions exhibit a significant DY suppression at large x_F , in clear disagreement with calculations including nPDF corrections only. This is the first time that the nuclear dependence of the DY process contradicts unambiguously nPDF expectations, indicating that other processes should be at work. This conclusion is confirmed by the direct comparison of E906 and E772/E866 results, which lack of x_2 scaling signals the violation of QCD factorization in Drell-Yan production in pA collisions.
- In contrast, the E906 results prove in good qualitative agreement with the energy loss model predictions, despite a slightly different magnitude, using the transport coefficient extracted from J/ψ data. This is a clear hint that energy loss in cold QCD matter affects the Drell-Yan process in nuclear collisions, while earlier claims of energy loss effects on DY production at higher collision energy

¹⁶parametrized by α , where α is defined as $\sigma(\text{pA} \rightarrow J/\psi \text{ X}) \equiv \sigma(\text{pp} \rightarrow J/\psi \text{ X}) \times A^\alpha$

¹⁷The suppression is much more pronounced in the J/ψ channel than in the DY process. Taking e.g. $\alpha = 0.75$ would lead to $R_{pA}^{J/\psi} \simeq 0.27$ in a $A = 200$ nucleus.

are spoiled by possible nPDF effects. Moreover, the qualitative agreement with E906 preliminary data points to a consistent value of the transport coefficient for two processes in two different dynamical regimes: LPM energy loss for Drell-Yan and fully coherent radiation for J/ψ .

- In π A collisions, energy loss effects are naturally smaller than in pA collisions due to the harder PDF in a pion with respect to that in a proton. However, it is shown that energy loss effects are of the same magnitude as nPDF corrections, sowing seeds of doubt on a clean extraction of nPDF from these data without including energy loss effects. Energy loss processes suppress the DY yield and helps reducing the known tension between nPDF results and NA10 data, however not sufficiently to claim for a good agreement. Predictions for the future COMPASS results are made; significant energy loss effects are expected especially above $x_F \gtrsim 0.7$ which should bring additional constraints on the cold nuclear matter transport coefficient.
- At E866 energy ($\sqrt{s} = 38.7$ GeV) the effects of LPM energy loss on DY production, using \hat{q} extracted from J/ψ data, significantly weaken, as already pointed out in Refs. [26, 45]. This justifies a posteriori the use of these results to extract nPDF, except at very large x_F where energy loss affects DY almost as much as nPDF corrections.

Acknowledgments

We would like to thank Yann Bedfer, Fabienne Kunne and Stéphane Peigné for a careful reading of the manuscript and for discussions. We also thank Po-Ju Lin for discussions on the E906 results. This work was supported in part by the P2IO LabEx (ANR-10-LABX-0038).

References

- [1] A. Majumder and M. Van Leeuwen, *The Theory and Phenomenology of Perturbative QCD Based Jet Quenching*, *Prog. Part. Nucl. Phys.* **66** (2011) 41 [[1002.2206](#)].
- [2] Y. Mehtar-Tani, J. G. Milhano and K. Tywoniuk, *Jet physics in heavy-ion collisions*, *Int. J. Mod. Phys.* **A28** (2013) 1340013 [[1302.2579](#)].
- [3] N. Armesto and E. Scapparini, *Heavy-ion collisions at the Large Hadron Collider: a review of the results from Run 1*, *Eur. Phys. J. Plus* **131** (2016) 52 [[1511.02151](#)].
- [4] G.-Y. Qin and X.-N. Wang, *Jet quenching in high-energy heavy-ion collisions*, *Int. J. Mod. Phys.* **E24** (2015) 1530014 [[1511.00790](#)].

- [5] F. Arleo, *Aspects of hard QCD processes in proton–nucleus collisions*, *Nucl. Part. Phys. Proc.* **289-290** (2017) 71 [[1612.07987](#)].
- [6] S. Peigné and A. Smilga, *Energy losses in a hot plasma revisited*, *Phys. Usp.* **52** (2009) 659 [[0810.5702](#)].
- [7] F. Arleo, S. Peigné and T. Sami, *Revisiting scaling properties of medium-induced gluon radiation*, *Phys. Rev.* **D83** (2011) 114036 [[1006.0818](#)].
- [8] F. Arleo and S. Peigné, *J/ψ suppression in pA collisions from parton energy loss in cold QCD matter*, *Phys. Rev. Lett.* **109** (2012) 122301 [[1204.4609](#)].
- [9] F. Arleo and S. Peigné, *Heavy-quarkonium suppression in pA collisions from parton energy loss in cold QCD matter*, *JHEP* **03** (2013) 122 [[1212.0434](#)].
- [10] F. Arleo, R. Koleyatov and S. Peigné, *Coherent medium-induced gluon radiation in hard forward $1 \rightarrow 1$ partonic processes*, *Phys. Rev.* **D93** (2016) 014006 [[1402.1671](#)].
- [11] S. Peigné and R. Koleyatov, *Medium-induced soft gluon radiation in forward dijet production in relativistic proton-nucleus collisions*, *JHEP* **01** (2015) 141 [[1405.4241](#)].
- [12] F. Arleo, R. Koleyatov, S. Peigné and M. Rustamova, *Centrality and p_\perp dependence of J/ψ suppression in proton-nucleus collisions from parton energy loss*, *JHEP* **05** (2013) 155 [[1304.0901](#)].
- [13] F. Arleo and S. Peigné, *Disentangling Shadowing from Coherent Energy Loss using the Drell-Yan Process*, *Phys. Rev.* **D95** (2017) 011502 [[1512.01794](#)].
- [14] R. Vogt, *The x_F dependence of ψ and Drell-Yan production*, *Phys. Rev.* **C61** (2000) 035203 [[hep-ph/9907317](#)].
- [15] E. Wang and X.-N. Wang, *Jet tomography of dense and nuclear matter*, *Phys. Rev. Lett.* **89** (2002) 162301 [[hep-ph/0202105](#)].
- [16] F. Arleo, *Quenching of hadron spectra in DIS on nuclear targets*, *Eur. Phys. J.* **C30** (2003) 213 [[hep-ph/0306235](#)].
- [17] **E772** collaboration, D. M. Alde et al., *Nuclear dependence of dimuon production at 800 GeV in the E772 experiment*, *Phys. Rev. Lett.* **64** (1990) 2479.
- [18] **E866** collaboration, M. A. Vasilev et al., *Parton energy loss limits and shadowing in Drell-Yan dimuon production*, *Phys. Rev. Lett.* **83** (1999) 2304 [[hep-ex/9906010](#)].
- [19] D. de Florian, R. Sassot, P. Zurita and M. Stratmann, *Global Analysis of Nuclear Parton Distributions*, *Phys. Rev.* **D85** (2012) 074028 [[1112.6324](#)].
- [20] K. Kovarik et al., *$n\text{CTEQ15}$ - Global analysis of nuclear parton distributions with uncertainties in the CTEQ framework*, *Phys. Rev.* **D93** (2016) 085037 [[1509.00792](#)].

- [21] K. J. Eskola, P. Paakkinen, H. Paukkunen and C. A. Salgado, *EPPS16: Nuclear parton distributions with LHC data*, *Eur. Phys. J.* **C77** (2017) 163 [[1612.05741](#)].
- [22] M. B. Johnson, B. Z. Kopeliovich, I. K. Potashnikova, P. L. McGaughey, J. M. Moss et al., *Energy loss versus shadowing in the Drell-Yan reaction on nuclei*, *Phys. Rev.* **C65** (2002) 025203 [[hep-ph/0105195](#)].
- [23] R. Neufeld, I. Vitev and B.-W. Zhang, *A possible determination of the quark radiation length in cold nuclear matter*, *Phys. Lett.* **B704** (2011) 590 [[1010.3708](#)].
- [24] L.-H. Song and L.-W. Yan, *Constraining the transport coefficient in cold nuclear matter with the Drell-Yan process*, *Phys. Rev.* **C96** (2017) 045203.
- [25] **NA3** collaboration, J. Badier et al., *Test of nuclear effects in hadronic dimuon production*, *Phys. Lett.* **B104** (1981) 335.
- [26] F. Arleo, *Constraints on quark energy loss from Drell-Yan data*, *Phys. Lett.* **B532** (2002) 231 [[hep-ph/0201066](#)].
- [27] **E906** collaboration, P. E. Reimer, *Drell-Yan Measurements by Fermilab E-906/SeaQuest*, <http://www.phy.anl.gov/mep/SeaQuest/> (2012) .
- [28] P.-J. Lin, *Measurement of Quark Energy Loss in Cold Nuclear Matter at Fermilab E906/SeaQuest*, <http://lss.fnal.gov/archive/thesis/2000/fermilab-thesis-2017-18.pdf>, Ph.D. thesis, Colorado U., 2017. 10.2172/1398791.
- [29] **COMPASS** collaboration, M. Aghasyan et al., *First measurement of transverse-spin-dependent azimuthal asymmetries in the Drell-Yan process*, *Phys. Rev. Lett.* **119** (2017) 112002 [[1704.00488](#)].
- [30] S. Catani and M. Grazzini, *An NNLO subtraction formalism in hadron collisions and its application to Higgs boson production at the LHC*, *Phys. Rev. Lett.* **98** (2007) 222002 [[hep-ph/0703012](#)].
- [31] S. Catani, L. Cieri, G. Ferrera, D. de Florian and M. Grazzini, *Vector boson production at hadron colliders: a fully exclusive QCD calculation at NNLO*, *Phys. Rev. Lett.* **103** (2009) 082001 [[0903.2120](#)].
- [32] L. A. Harland-Lang, A. D. Martin, P. Motylinski and R. S. Thorne, *Parton distributions in the LHC era: MMHT 2014 PDFs*, *Eur. Phys. J.* **C75** (2015) 204 [[1412.3989](#)].
- [33] S. Dulat, T.-J. Hou, J. Gao, M. Guzzi, J. Huston et al., *New parton distribution functions from a global analysis of quantum chromodynamics*, *Phys. Rev.* **D93** (2016) 033006 [[1506.07443](#)].

- [34] M. Glück, E. Reya and A. Vogt, *Pionic parton distributions*, *Z. Phys.* **C53** (1992) 651.
- [35] P. J. Sutton, A. D. Martin, R. G. Roberts and W. J. Stirling, *Parton distributions for the pion extracted from Drell-Yan and prompt photon experiments*, *Phys. Rev.* **D45** (1992) 2349.
- [36] P. C. Barry, N. Sato, W. Melnitchouk and C.-R. Ji, *First Monte Carlo global QCD analysis of pion parton distributions*, [1804.01965](#).
- [37] R. Baier, Y. L. Dokshitzer, A. H. Mueller and D. Schiff, *Quenching of hadron spectra in media*, *JHEP* **09** (2001) 033 [[hep-ph/0106347](#)].
- [38] F. Arleo, *Tomography of cold and hot QCD matter: Tools and diagnosis*, *JHEP* **11** (2002) 044 [[hep-ph/0210104](#)].
- [39] C. A. Salgado and U. A. Wiedemann, *Calculating quenching weights*, *Phys. Rev.* **D68** (2003) 014008 [[hep-ph/0302184](#)].
- [40] R. Baier, Y. L. Dokshitzer, A. H. Mueller, S. Peigné and D. Schiff, *Radiative energy loss and p_{\perp} broadening of high energy partons in nuclei*, *Nucl. Phys.* **B484** (1997) 265 [[hep-ph/9608322](#)].
- [41] M. Gyulassy, P. Levai and I. Vitev, *Jet quenching in thin quark gluon plasmas. 1. Formalism*, *Nucl. Phys.* **B571** (2000) 197 [[hep-ph/9907461](#)].
- [42] X.-N. Wang and X. Guo, *Multiple parton scattering in nuclei: Parton energy loss*, *Nucl. Phys.* **A696** (2001) 788 [[hep-ph/0102230](#)].
- [43] S. J. Brodsky and G. R. Farrar, *Scaling Laws at Large Transverse Momentum*, *Phys. Rev. Lett.* **31** (1973) 1153.
- [44] NA10 collaboration, P. Bordalo et al., *Nuclear Effects on the Nucleon Structure Functions in Hadronic High Mass Dimuon Production*, *Phys. Lett.* **B193** (1987) 368.
- [45] H. Xing, Y. Guo, E. Wang and X.-N. Wang, *Parton Energy Loss and Modified Beam Quark Distribution Functions in Drell-Yan Process in $p+A$ Collisions*, *Nucl. Phys.* **A879** (2012) 77 [[1110.1903](#)].
- [46] W.-t. Deng and X.-N. Wang, *Multiple Parton Scattering in Nuclei: Modified DGLAP Evolution for Fragmentation Functions*, *Phys. Rev.* **C81** (2010) 024902 [[0910.3403](#)].
- [47] P. Paakkinen, K. J. Eskola and H. Paukkunen, *Applicability of pion nucleus Drell-Yan data in global analysis of nuclear parton distribution functions*, *Phys. Lett.* **B768** (2017) 7 [[1609.07262](#)].
- [48] P. Hoyer, M. Vanttinen and U. Sukhatme, *Violation of factorization in charm hadroproduction*, *Phys. Lett.* **B246** (1990) 217.

- [49] Y. H. Leung, *PHENIX measurements of charm, bottom, and Drell-Yan via dimuons in pp and pAu at $\sqrt{s_{NN}} = 200$ GeV*, <https://indico.cern.ch/event/634426/contributions/3090546/attachments/1727756/2791469/hp2018vf.pdf> (2018) .
- [50] **LHCb** collaboration, I. Bediaga et al., *Physics case for an LHCb Upgrade II - Opportunities in flavour physics, and beyond, in the HL-LHC era*, [1808.08865](#).
- [51] **NA3** collaboration, J. Badier et al., *Experimental J/ψ Hadronic Production from 150 GeV/c to 280 GeV/c*, *Z. Phys.* **C20** (1983) 101.
- [52] **E866** collaboration, M. J. Leitch et al., *Measurement of differences between J/ψ and ψ' suppression in pA collisions*, *Phys. Rev. Lett.* **84** (2000) 3256 [[nucl-ex/9909007](#)].
- [53] **PHENIX** collaboration, A. Adare et al., *Cold Nuclear Matter Effects on J/ψ Yields as a Function of Rapidity and Nuclear Geometry in Deuteron-Gold Collisions at $\sqrt{s_{NN}} = 200$ GeV*, *Phys. Rev. Lett.* **107** (2011) 142301 [[1010.1246](#)].
- [54] **ALICE** collaboration, B. B. Abelev et al., *J/ψ production and nuclear effects in pPb collisions at $\sqrt{s_{NN}} = 5.02$ TeV*, *JHEP* **1402** (2014) 073 [[1308.6726](#)].
- [55] **LHCb** collaboration, R. Aaij et al., *Prompt and nonprompt J/ψ production and nuclear modification in pPb collisions at $\sqrt{s_{NN}} = 8.16$ TeV*, *Phys. Lett.* **B774** (2017) 159 [[1706.07122](#)].
- [56] M. Leitch, *Overview of charm physics at RHIC*, *AIP Conf.Proc.* **892** (2007) 404 [[nucl-ex/0610031](#)].